

# Selective Detection of NO<sub>2</sub> with Specific Filters for O<sub>3</sub> Trapping †

Mehdi Othman <sup>1</sup>, Christophe Théron <sup>2</sup>, Marc Bendahan <sup>1</sup>, Charles Rivron <sup>2</sup>, Sandrine Bernardini <sup>1</sup>, Guillaume Le Chevallier <sup>2</sup>, Ludovic Caillat <sup>2</sup>, Khalifa Aguir <sup>1,\*</sup> and Thu-Hoa Tran-Thi <sup>2</sup>

<sup>1</sup> Aix Marseille Univ, Université de Toulon, CNRS, IM2NP, 13397 Marseille, France;

mehdi.othman@im2np.fr (M.O.); marc.bendahan@im2np.fr (M.B.); sandrine.bernardini@im2np.fr (S.B.)

<sup>2</sup> NIMBE, CEA, CNRS, Université Paris-Saclay, CEA-Saclay, 91191 Gif sur Yvette Cedex, France;

christophe.theron@cea.fr (C.T.); charles.rivron@cea.fr (C.R.); guillaume.le-chevallier@cea.fr (G.L.C.);

ludovic.caillat@cea.fr (L.C.); thu-hoa.tran-thi@cea.fr (T.-H.T.-T.)

\* Correspondence: khalifa.aguir@im2np.fr; Tel.: +33-(0)491-288-972

† Presented at the EuroSensors 2017 Conference, Paris, France, 3–6 September 2017.

Published: 28 August 2017

**Abstract:** The present study evaluates the ozone (O<sub>3</sub>) and nitrogen dioxide (NO<sub>2</sub>) removal performance of specific filters based on nanoporous materials. These materials, produced via the sol-gel process with functionalized silicon alkoxides as precursors, are tailored for O<sub>3</sub> trapping. The gas removal effectiveness of the filters was assessed through measurements of O<sub>3</sub> concentrations in the air upstream and downstream of the filters. Depending on the filter nature, O<sub>3</sub> can be totally trapped while NO<sub>2</sub> can pass over a specific concentration range.

**Keywords:** selective filter; gas sensors; trapping efficiency; ozone; nitrogen dioxide

## 1. Introduction

The Tropospheric or ground level ozone (O<sub>3</sub>) is an air pollutant produced by photochemical reactions and chemical reactions between oxides of nitrogen (NO<sub>x</sub>) and volatile organic compounds (VOC). High outdoor O<sub>3</sub> concentrations have been linked to asthma exacerbation, respiratory symptoms, heart attacks and premature death. In addition to the direct health risks, O<sub>3</sub> can also chemically react with various indoor pollutants [1,2] to produce more toxic volatile compounds. Since O<sub>3</sub> is the main interfering pollutant for NO<sub>2</sub> monitoring in the context of air quality control, various filters (nanocarbon, indigo thin film or MnO<sub>2</sub>) were proposed and were found to efficiently trap O<sub>3</sub> without trapping NO<sub>2</sub> [3,4]. However, due to their structure, these filters were found to be too short-lived. Thus, our approach consists in the implementation of a relevant chemical filter highly impervious to O<sub>3</sub> and weakly reactive with NO<sub>2</sub> placed upstream a MOX gas sensors.

Various filters have been investigated based on several functionalized nanoporous materials doped with indigo carmine for the selective trapping of O<sub>3</sub>. The filtering efficiency towards the target gases have been experimentally quantified for the different gas concentrations.

The work presented in this paper is divided into two parts; firstly, we describe the strategy of producing various filters with functionalized nanoporous matrices via the sol-gel process. Then, the synthesized filters will be tested in order to quantify their ability of O<sub>3</sub> trapping under various conditions. The second part is dedicated to the selection of filters to be used for NO<sub>2</sub> detection in O<sub>3</sub> environment. Various tests have been performed to check the total O<sub>3</sub> trapping by the filters with sensor and NO<sub>2</sub> detection with WO<sub>3</sub> based gas sensor using various O<sub>3</sub> up-stream filters.

## 2. Experimental

### 2.1. Syntheses of Doped Nanoporous Matrices and Characterization

Nanoporous monoliths of hybrid organic-inorganic polymers doped with indigo carmine were prepared via the Sol-Gel method using as reactants one or two silicon precursors. A one-pot synthesis procedure is applied for all syntheses. The chosen silicon precursors are tetramethoxy silane (TMOS), phenyl-triethoxysilane (PhTEOS) and chloropropyl-trimethoxysilane (CITMOS). TMOS or a mixture of TMOS with either PhTEOS or CITMOS are added to the solvent, MeOH, in a beaker and the mixture is vigorously stirred while adding an aqueous solution of indigo carmine. The concentration of indigo carmine in the aqueous solution,  $70 \text{ g}\cdot\text{L}^{-1}$ , corresponds to its solubility in water. The sol was poured into specific molds where gelation occurs. The gels were dried in a desiccator under a  $\text{N}_2$  stream at room temperature. After the shrinkage process, transparent and dark blue monoliths were obtained. The proportion of the reactants is given in Table 1 along with the drying time.

**Table 1.** Synthesis conditions and porosity properties of the matrices doped with indigo carmine (IC). [IC] corresponds to the concentration in the Sol.

Filter	Sol Composition Molar Proportion	[IC] mol·L <sup>-1</sup>	Drying Time Days	Sads m <sup>2</sup> ·g <sup>-1</sup>	V3 cm <sup>3</sup> ·g <sup>-1</sup>
F1	TMOS/PhTEOS/MeOH/H <sub>2</sub> O 0.85/0.15/4/4	0.0266	38	560 ± 50 34% (11–20 Å), 66% (21–53 Å)	0.38 ± 0.01
F2	TMOS/CITMOS/MeOH/H <sub>2</sub> O 0.8/0.2/4/4	0.0271	38	8 ± 2 100% (25–70 Å)	0.01
F3	TMOS/CITMOS/MeOH/H <sub>2</sub> O 0.5/0.5/4/4	0.0263	32	Non porous	-
F4	TMOS/CITMOS/MeOH/H <sub>2</sub> O 0.7/0.3/4/4	0.0304	15	Non porous	-

The concentration of indigo carmine in the final matrices varies from 0.280 to 0.324 mol·cm<sup>-3</sup>, depending on the formulation. The porosity parameters, specific adsorption surface area and pore volume were determined via collecting adsorption isotherms of  $\text{N}_2$  at liquid nitrogen temperature with a porosity analyzer, Autosorb-1 from Quantachrome Instruments. F1 displays the highest specific adsorption surface area due to the presence of 34% of micropores (diameter < 20 Å) while F2 displays only mesopores (500 > diameter > 20 Å). The materials listed in Table 1 are ground, sieved and transferred into syringes of 3 mm of diameter. Each filter is filled with 1.79 g of the material to be tested.

### 2.2. Experimental Set-Up for the Detection of O<sub>3</sub> and NO<sub>2</sub>

The sensor used in this study consists of a new microhotplate platform and a sensitive layer. The microhotplate architecture was initially developed by IM2NP laboratory [5]. A thin dielectric membrane of 450 μm × 430 μm supports a set of three sensors and two heaters. A platinum heaters was designed to ensure the optimum response of the sensitive layer (Figure 1). In addition, two pairs of Pt electrodes were deposited on the same mask level and used to recover the signal on the sensitive layer. The metal-oxide is a polycrystalline WO<sub>3</sub> sensitive layer (50 nm thick) produced by reactive R.F (13.56 MHz) magnetron sputtering and can detect both O<sub>3</sub> and NO<sub>2</sub>. The gas sensing response is obtained by measuring the microsensor resistance with a Keithley 2450 source meter. The sensor is placed in a close thermo-regulated test chamber. The sensor sensitivity to NO<sub>2</sub> and O<sub>3</sub> is studied under several pollutant concentrations, from 200 ppb to 1000 ppb for NO<sub>2</sub> and from 36 ppb to 210 ppb for O<sub>3</sub>. The experimental setup allows the tests of sensors under dry air and various calibrated gas mixtures, without or with the up-stream filter. For each pollutant concentration, the sensor was exposed to the gas mixture with constant flow rate of 500 sccm.

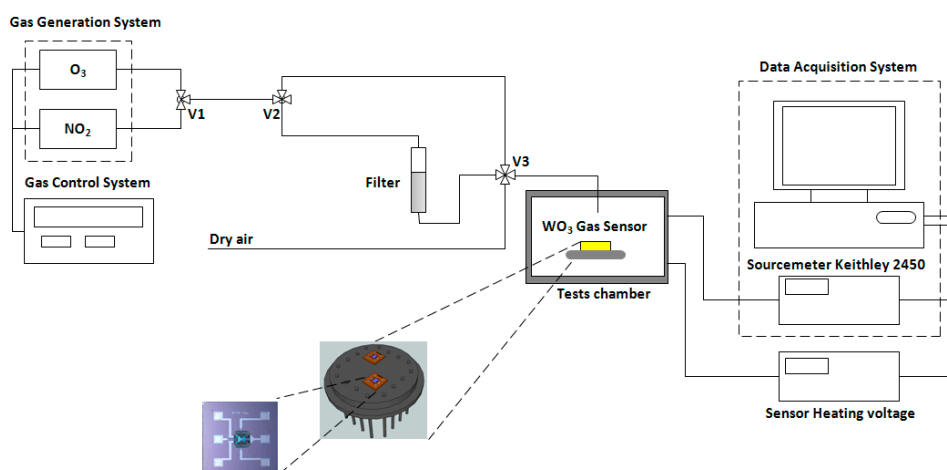


**Figure 1.** Experimental setup for gas sensors and filters tests.

The trapping efficiency,  $\tau$ , corresponds to the amount of gas removed and is expressed in % (Equation (1)).  $\tau$  is measured for each filter as a function of the exposure parameters.

$$\tau = \frac{[gas]_{up} - [gas]_{down}}{[gas]_{up}} 100\% \quad (1)$$

### 3. Results and Discussion

In order to evaluate the efficiency of O<sub>3</sub> and NO<sub>2</sub> trapping, different measurements were carried out for each filter filled with 1.79 g of filtering material and placed up-stream of the WO<sub>3</sub>-based sensor. F1 and F2 filters were found to remove completely O<sub>3</sub> but not NO<sub>2</sub> as shown in Table 2. In contrast, F3 and F4 which display no porosity only partially remove O<sub>3</sub> and NO<sub>2</sub>.

**Table 2.** Filter trapping performance under O<sub>3</sub> and NO<sub>2</sub>.

Filter	O <sub>3</sub>	NO <sub>2</sub>
F1	✓	✗
F2	✓	✗
F3	✗	✗
F4	✗	✗

✓: removes completely the gas molecules; ✗: does not completely remove the gas molecules.

The efficiency of the filters in removing O<sub>3</sub> is further tested with reduced amounts of filtering material (0.2 g). As shown in Figure 2a, F1 and F2 can still completely eliminate O<sub>3</sub> molecules while only a part of the initial concentration is removed with F3 and F4. For these latter, it can also be noted that the O<sub>3</sub> removal is increased with increasing O<sub>3</sub> concentration. In other terms, this means that the O<sub>3</sub> amount passing through the filter decreases as the up-stream concentration O<sub>3</sub> increases.

On the other hand, and unlike the O<sub>3</sub> case, all the filters remove partially NO<sub>2</sub> as illustrated in Figure 2b and the NO<sub>2</sub> removal appears to be dependent on the up-stream NO<sub>2</sub> concentration.

These preliminary results clearly indicate that F1 and F2 can efficiently trap O<sub>3</sub> and could be used to measure NO<sub>2</sub> in gas mixtures containing both pollutants. Further experiments will be needed to find out the range of NO<sub>2</sub> concentration over which F1 and F2 could be used up-stream of the sensor for the measurements of NO<sub>2</sub> in air.

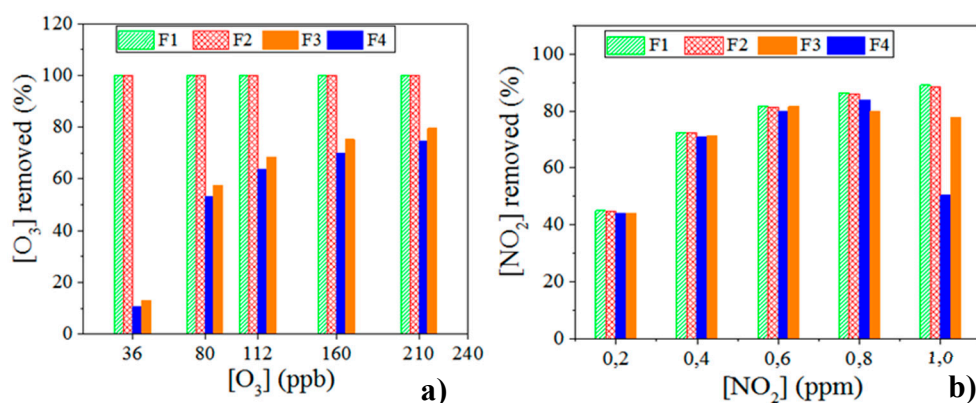


**Figure 2.** Amount of gas removed by the four filters F1, F2, F3 and F4 as a function of initial concentration: (a) under O<sub>3</sub> and (b) under NO<sub>2</sub>.

This work will also be enriched with future experiments combining humidity, gas mixture and filter. These ongoing experiments will allow to define the best conditions of use of filters coupled to the microsensors.

**Acknowledgments:** This research is supported by bpi-France in the framework of the SMARTY Project (Smart AiR qualiTY). The authors gratefully acknowledge A. Combes and T. Fiorido, from the IM2NP, for their technical assistance.

**Conflicts of Interest:** The authors declare no conflict of interest.

## References

1. Weschler, C.J. Ozone's impact on public health: Contributions from indoor exposures to ozone and products of ozone-initiated chemistry. *Environ. Health Perspect.* **2006**, *114*, 1489–1496.
2. Apte, M.G.; Buchanan, I.S.; Mendell, M.J. Outdoor ozone and building-related symptoms in the base study. *Indoor Air* **2008**, *18*, 156–170.
3. Brunet, J.; Dubois, M.; Pauly, A.; Spinelle, L.; Ndiaye, A.; Guérin, K.; Varenne, C.; Lauron, B. An innovative gas sensor system designed from a sensitive organic semiconductor downstream a nanocarbonaceous chemical filter for the selective detection of NO<sub>2</sub> in an environmental context. Part I: Development of a nanocarbon filter for the removal of ozone. *Sens. Actuator B Chem.* **2012**, *173*, 659–667.
4. Viricelle, J.-P.; Pauly, A.; Mazet, L.; Brunet, J.; Bouvet, M.; varenne, C.; Pijolat, C. Selectivity improvement of semi-conducting gas sensors by selective filter for atmospheric pollutants detection. *Mater. Sci. Eng. C Elsevier* **2006**, *26*, 186–195.
5. Aguir, K.; Bendahan, M.; Laithier, V. Heated Sensitive Layer Gas Sensor. U.S. Patent, 20160238548 A1, 18 August 2016.



© 2017 by the authors. Licensee MDPI, Basel, Switzerland. This article is an open access article distributed under the terms and conditions of the Creative Commons Attribution (CC BY) license (<http://creativecommons.org/licenses/by/4.0/>).